The Canadian Mineralogist
Vol. 36, pp. 1217-1223 (1998)

RAMAN AND INFRARED SPECTRA OF PHASE E, A PLAUSIBLE HYDROUS PHASE IN THE MANTLE

TERRENCE P. MERNAGH[1]

Australian Geological Survey Organisation, GPO Box 378, Canberra, ACT, 2601, Australia

LIN-GUN LIU

Institute of Earth Sciences, Academia Sinica, Taipei, Taiwan 115

Abstract

Micro-Raman and micro-infrared spectra of the silicate and principal OH-stretching regions have been obtained from a well-characterized crystal of phase E ($Mg_{2.17}Si_{1.01}H_{3.62}O_6$) containing approximately 18 wt.% H_2O. The number of observed infrared and Raman bands exceeds the number predicted by factor-group analysis for a crystal of phase E with space group $R\bar{3}m$. This finding suggests that some long-range order may exist in phase E, or that it possesses a superstructure that lowers the overall symmetry of the crystal. Although phase E contains layers of brucite-type units linked by SiO_4 tetrahedra and MgO_6 octahedra, the lower frequencies and the broadness of the OH-stretching bands of phase E (in comparison to brucite) indicate that the hydrogen bonding is stronger than that in brucite. There is a close similarity between the Raman spectra of phase E and forsterite below 1000 cm^{-1}. This may be explained by assuming that the vibrations of the isolated SiO_4 tetrahedra dominate the Raman spectrum of phase E below 1000 cm^{-1}. Tentative assignments of the observed bands are made by comparison with computed spectral modes and the corresponding spectra of brucite and forsterite.

Keywords: hydrous magnesium silicate, phase E, micro-Fourier-transform infrared spectroscopy, micro-Raman spectroscopy, mantle.

Sommaire

Nous avons obtenu des spectres micro-Raman et micro-infrarouges de la trame silicatée et des principales régions d'étirement des groupes OH d'un cristal bien caractérisé de la phase E ($Mg_{2.17}Si_{1.01}H_{3.62}O_6$), contenant environ 18% de H_2O par poids. Le nombre de bandes Raman et infrarouges observé dépasse ce que nous prédisons selon l'analyse des groupes et facteurs pour un cristal de cette phase dans le groupe spatial $R\bar{3}m$. La phase E serait donc ordonnée à longue échelle, ou bien elle aurait une surstructure qui réduit la symétrie globale du cristal. Quoique la phase E contient des couches de type brucite liées par des tétraèdres SiO_4 et des octaèdres MgO_6, les fréquences plus faibles et la largeur des bandes d'étirement des groupes OH, en comparison de celles-ci dans la brucite, montrent que les liaisons hydrogène sont ici plus fortes que dans la brucite. Le spectre Raman de la phase E dans l'intervalle inférieur à 1000 cm^{-1} ressemble beaucoup à celui de la forstérite. Les vibrations des tétraèdres isolés de SiO_4 domineraient donc le spectre Raman de la phase E aux fréquences inférieures à 1000 cm^{-1}. Nous identifions les bandes observées de façon préliminaire par comparaison avec les modes calculés et avec les spectres correspondants de la brucite et de la forstérite.

(Traduit par la Rédaction)

Mots-clés: silicate hydraté de magnésium, phase E, spectroscopie infra-rouge avec transformation micro-Fourier, spectroscopie micro-Raman, manteau.

Introduction

There is currently considerable interest in the state of hydration of the mantle. Liu (1987) has estimated that the Earth's mantle might contain more than five times the present content of H_2O in the hydrosphere and crust. In order to hold this amount of H_2O inside the Earth, there must be some magnesium silicates that can accommodate it and that are stable at appropriate pressures and temperatures. In addition to the three hydrous magnesium silicates (phases A, B and C), synthesized by Ringwood & Major (1967), there are several other dense hydrous magnesium silicates (*e.g.*, phase D: Liu 1987).

[1] *E-mail address*: terry.mernagh@agso.gov.au

Phase E was first reported by Kanzaki (1989, 1991) as part of a study of phase equilibria of hydrous materials at pressures above 120 kbar. Phase E is generally formed in the range 130–155 kbar and 1000–1200°C, and hence, may be stable at depths ranging from the lower regions of the upper mantle to the transition zone. X-ray- and electron-diffraction studies (Kudoh *et al.* 1993) showed that phase E has a cation-disordered structure with a rhombohedral arrangement of layers of brucite-type units. The layers are cross-linked by silicon in tetrahedral coordination, magnesium in octahedral coordination, and hydrogen bonds. Interlayer octahedra share edges with intralayer octahedra. Interlayer tetrahedra would be expected to share faces with intralayer octahedra, but to avoid this, there are vacancies within the layers. Kudoh *et al.* (1993) suggested that there is no long-range order in phase E, Mg and Si being distributed statistically throughout an essentially close-packed arrangement of oxygen atoms.

The Raman-active OH-stretching bands of phase E were recently reported by Ohtani *et al.* (1995) and the first complete Raman spectrum of phase E was published by Liu *et al.* (1997). In this paper, we examine the Raman spectrum of phase E in more detail and compare it to the corresponding infrared spectrum of the same sample.

Experimental

Single crystals of phase E (~100 μm diameter) were synthesized at 155 kbar and 1200°C for 22 minutes by Inoue *et al.* (1995) and at 150 kbar and 1000°C for 3 hours in the present study. The crystal structure of samples synthesized in the present study was confirmed by a micro-focus X-ray diffractometer. Electron-microprobe analysis of the samples synthesized in the present study gave Mg/Si = 1.90 ± 0.02, and the amount of H_2O, 18.2 ± 0.9 wt.%, was estimated by difference. The amounts of H_2O in two different samples of phase E were estimated to be 15.8 and 18.0 wt.% by Kudoh *et al.* (1993) on the basis of X-ray crystal-structure analysis, giving compositions of $Mg_{2.08}Si_{1.16}H_{3.20}O_6$ and $Mg_{2.17}Si_{1.01}H_{3.62}O_6$, respectively.

Fourier-transform infrared (FTIR) spectra were recorded from 750 to 4000 cm^{-1} using a Bomen infrared spectrometer and a Spectra-Tech microscope. FTIR spectra were obtained at 4 cm^{-1} resolution by addition of 500 scans for each sample and reference spectrum. To ensure that only the spectrum of the crystal was obtained, a rectangular region of approximately 30 × 20 μm was selected for analysis by masking the image at an intermediate focal plane within the microscope. Polarized spectra could not be obtained owing to the small size of the crystal used in these studies and the depolarizing effects caused by the microscope objective.

Raman spectra were recorded on a Microdil 28 spectrometer equipped with an Olympus BH2 microscope. A 100× microscope objective was used to focus the laser beam to a spot about 1 μm in diameter on the crystal. A complete description of the Raman instrumentation is given in Liu & Mernagh (1990). Spectra were measured at approximately 3 cm^{-1} resolution from 150 to 3800 cm^{-1} using 514.5 nm excitation and 40 mW power at the sample. All spectra were obtained after 15 accumulations using a 15-s integration time. Raman peaks are accurate to ±1 cm^{-1}, except for the broader OH bands, which are accurate to ±5 cm^{-1}.

Results and Discussion

Predicted vibrational spectra for phase E

The X-ray- and electron-diffraction studies of Kudoh *et al.* (1993) indicate that phase E has a hexagonal unit-cell with space group $R\bar{3}m$. However, in order to develop a plausible crystal-structure, Kudoh *et al.* (1993) proposed that occupied Si tetrahedra cannot share faces with occupied intralayer Mg octahedra. Therefore, all three cation positions (Mg1, Mg2 and Si) are only partly occupied. The pattern of vacancies and interlayer cations is ordered locally, but has no long-range order. In order to simplify the modeling, only the short-range structure will currently be considered, and hence, a factor-group analysis based on the $R\bar{3}m$ space group predicts the following irreducible representation for phase E:

$$\Gamma = 3\ A_{1g} + 3\ E_g + 4\ A_{2u} + 4\ E_u$$

Thus, a total of 14 vibrational modes are predicted for this structure. Owing to the centrosymmetry of the space group $R\bar{3}m$, the mutual exclusion rule for normal vibrations in a crystal requires that the u-modes be active in the infrared spectrum and the g-modes be active in the Raman spectrum only.

In order to make band assignments for the observed infrared and Raman spectra of phase E, the VIBRATZ program, a new version of the modeling software by Dowty (1987a), was used to calculate the vibrational frequencies of phase E and to refine the data based on the observed infrared and Raman spectra. The VIBRATZ program requires, as input, the unit-cell parameters and space group, the location of one atom of each equivalent set, obtained from Table 1 in Kudoh *et al.* (1993), the atomic coordinates of the general equipoint, and a set of force constants that apply to conventional two-atom bonds, three-atom angles, four-atom torsion or bond-plane angles, and interactions of bonds and three-atom angles.

The initial force constants for the Si–O and Mg–O bonds were obtained from Table 2 of Dowty (1987b), and the O–H force constant was obtained from Table 8–1 in Wilson *et al.* (1980). The bond lengths of Kudoh *et al.* (1993) were used in these calculations. As Kudoh *et al.* (1993) could not determine the length of the O–H bond in their X-ray studies, the bond length of O–H in brucite (0.96 Å), determined by neutron-diffraction

TABLE 1. A COMPARISON OF CALCULATED AND OBSERVED VIBRATIONAL FREQUENCIES FOR PHASE E

Calculated Frequencies (cm^{-1})	Observed Frequencies (cm^{-1})	Mode Assignments	Calculated Frequencies (cm^{-1})	Observed Frequencies (cm^{-1})	Mode Assignments
3802	3642	A_{2u}		819	
3686	3616	A_{1g}		814	
	3598			717	
3175	3368	E_u	698	678	E_u
2949	3331	E_g		584	
	1575		460	541	A_{1g}
	1439		351	432	A_{2u}
	955		306	418	E_u
840	906	E_g	342	322	E_g
899	888	A_{1g}	225	288	E_u
716	846	A_{2u}	221	221	A_{2u}

studies (Catti *et al.* 1995), was used in view of the similarities between the crystal structure of phase E and brucite.

A comparison of the frequencies of phase E calculated by VIBRATZ with those observed in the present study is given in Table 1. The calculated frequencies have an average deviation of less than 10% from the observed values. Although there are some differences between the calculated and observed values, it is important to remember that the calculated values are harmonic, whereas the observed values are essentially anharmonic. These calculations also have not considered the Mg and Si vacancies invoked by Kudoh *et al.* (1993), for reasons mentioned above.

Note that the number of observed bands exceeds the number predicted from the above factor-group analysis, and that some Raman bands seem to coincide with observed and predicted infrared modes. This observation suggests that some long-range order may exist in phase E, or that it has a superstructure that lowers the overall symmetry of the crystal, resulting in an increase in the number of vibrational bands in the spectra. These results conflict with the selected-area electron diffraction (SAED) patterns obtained by Kudoh *et al.* (1993), which indicate that phase E does not possess any long-range superstructure. However, their interpretation was based solely on the similarities between the diffuse scattering in the SAED and that observed in short-range-ordered alloys. Some possible reasons for the additional bands and tentative assignments are given below.

Micro-FTIR spectrum

The micro-FTIR spectrum of phase E is shown in Figure 1, and the observed frequencies are listed in Table 2. Two strong Si–O stretching bands are observed at 819 and 955 cm^{-1}, with a slight shoulder at 888 cm^{-1}. The two bands at 1439 and 1575 cm^{-1} occur outside the range of normal Si–O vibrations, and are probably overtones or combination bands. The features in the spectrum between 2330 and 2360 cm^{-1} are due to a slight decrease in the concentration of CO_2 between the recording of the background and sample spectra, and other weak features below 3000 cm^{-1} may be overtones or combination bands.

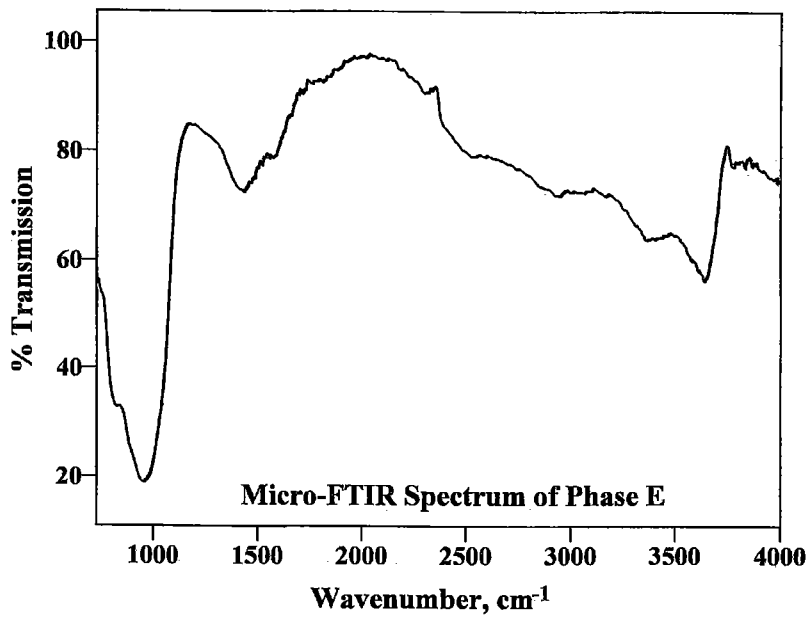

FIG. 1. Unpolarized micro-FTIR spectrum in the region 750 to 4000 cm^{-1} recorded from a single crystal of phase E.

TABLE 2. THE OBSERVED INFRARED AND RAMAN BANDS* OF PHASE E AND FORSTERITE

Phase E		Forsterite			Assignments
FTIR[a]	Raman[a]	Infrared[b] υ_{TO}	Infrared[b] υ_{LO}	Raman[c]	
	221	224		226	SiO_4 translation
	288	280	283	286	mixed (SiO_4 translation)
	322	320	323	323	mixed mode
	418	421	446	422	υ_2
	432			434	υ_2
	541	498	544	545	υ_4
	584	502	585	582	υ_4
	717				O-H rotation
819	814	825		824	$\upsilon_1 + \upsilon_3$
	846	838	845	856	$\upsilon_1 + \upsilon_3$
888		885	994		υ_3
	906			920	υ_3
955	949	957	963	965	υ_3
1439					combination/overtone
1575					combination/overtone
	3331				O-H stretch
3368					O-H stretch
	3616				O-H stretch
3642					O-H stretch

* All frequencies are quoted in cm^{-1}. a. This study. b. Selected infrared frequencies of forsterite from Iishi (1978). c. Selected Raman frequencies of forsterite from Chopelas (1991).

The two very broad bands at 3368 and 3642 cm^{-1} in the principal OH-stretching region of Figure 1 indicate that either H_2O or weakly bonded OH, or both, are present in phase E. This proposal is in accord with the results of the electron-microprobe analysis, which indicate that up to 18 wt.% H_2O may be present in phase E. Despite the fact that phase E contains brucite-like layers, all the OH-stretching bands occur at lower frequencies than the relatively sharp OH-stretching band of brucite at 3695–3698 cm^{-1} (Liese 1975, Table II). Both the lower frequencies and the broadness of the OH- stretching bands indicate that the hydrogen bonding in phase E is stronger than that in brucite.

Figure 2 shows an expanded view of the principal OH-stretching for phase E. An approximate value of 100 $L.mol^{-1}.cm^{-1}$ may be used for the absorptivity of the fundamental OH-stretching vibration in minerals (Rossman 1988) in order to estimate the OH content. An average (2.83 $g.cm^{-3}$) of the densities for phase E given in Kudoh *et al.* (1993) was used in these calculations. Thus by integrating the OH-stretching bands in the infrared spectrum of Figure 2 and using an estimated thickness of 100 μm, the calculated concentration of OH is 20% by weight. Considering the assumptions made in these calculations, this result is in good agreement with the results of the electron-microprobe analysis (H_2O calculated by difference) mentioned above.

Micro-Raman spectrum

The complete Raman spectrum of phase E is shown in Figure 3. Note that the three bands between 1000 and 3000 cm^{-1} are due to remnants of a previous carbon coating on the sample, which could not be removed owing to the small size of the crystal. In the principal OH-stretching region, there is one strong band at 3616

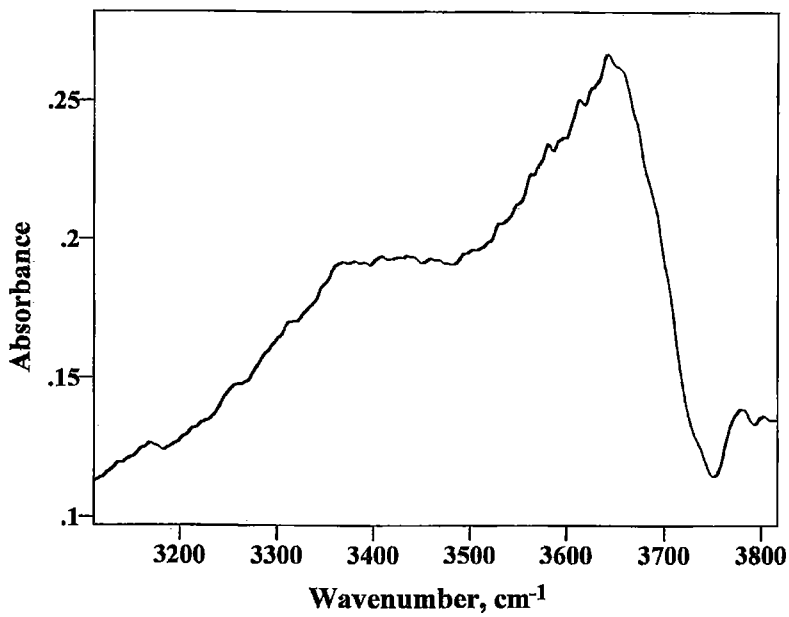

FIG. 2. An unpolarized FTIR spectrum of the principal OH-stretching region of phase E.

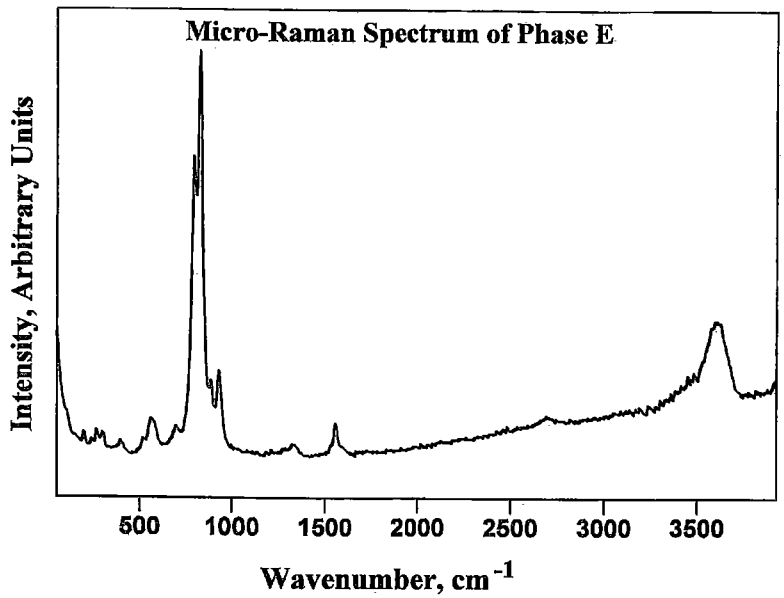

FIG. 3. Micro-Raman spectrum in the region 100 to 3800 cm^{-1} recorded from a single crystal of phase E. Note that the bands between 1000 and 3000 cm^{-1} are due to remnants of a carbon coating on the sample from previous studies (see text for further explanation).

cm^{-1} and a weak, broad shoulder on the low-frequency side of this band. The profile of the Raman OH-stretching bands is somewhat similar to those of the infrared spectrum (Figs. 1, 2), although the band at lower wavenumbers is not as pronounced in the Raman spectrum. It is worth noting that a new peak was also observed on the high-frequency side of the Raman OH-stretching mode of brucite in the high-pressure study of Duffy *et al.* (1995). According to these authors, the coinciding bands may be due to mixing of formally infrared and Raman modes due to structural distortion or disorder.

Both the Raman OH-stretching bands of phase E occur at considerably lower wavenumber than the A_{1g} OH-stretching mode for brucite, at 3652 cm^{-1} (Duffy *et al.* 1995). The higher strength of hydrogen bonding in phase E is shown by the shift to lower wavenumber and by the greater width of the bands in the ambient Raman spectrum. Although phase E is reported to contain layers of brucite-type units (Kudoh *et al.* 1993), the Raman spectrum contains several intense bands in the low-frequency region above 800 cm^{-1} that are not observed in the Raman spectrum of brucite (Duffy *et al.* 1995). However, the weak bands at 288, 432 and 717 cm^{-1} (Fig. 3) may correspond to vibrations of brucite-type units, as they all lie within 8–11 cm^{-1} of the reported Raman-active modes of brucite. The Raman-active vibrations of the brucite-like layers are relatively weak, a common feature of many silicates, *e.g.*, pyroxenes (Mernagh & Hoatson 1997). This is due to the predominantly ionic nature of the MgO_6 octahedra (Farmer 1974).

It is interesting to note, however, the close similarity of the Raman spectra of phase E and forsterite below 1000 cm^{-1} (Fig. 4). Comparison of the observed infrared and Raman frequencies of phase E with those of forsterite (Table 2) shows that the Raman bands of phase E occur at slightly lower wavenumber than those of forsterite. A similar relation occurs for the Raman spectra of β-Mg_2SiO_4 and the hydrous β-phase (Mernagh & Liu 1996). Although phase E and forsterite have quite different structures, they both contain individual SiO_4 tetrahedra. Thus, it seems that the vibrations of SiO_4 tetrahedra dominate the Raman spectrum of phase E below 1000 cm^{-1}.

The inference that many of the observed Raman modes (particularly those between 800 and 1100 cm^{-1}) are due to SiO_4 vibrations is supported by the results of Paques-Ledent & Tarte (1973) on forsterite containing varying $^{28}Si/^{30}Si$ and $^{24}Mg/^{26}Mg$ ratios. They found that bands in the range 800–1100 cm^{-1} are not affected by the proportion of Mg-isotopes, indicating that little or no Mg translations are involved in these high-frequency modes. However, the bands between 991 and 885 cm^{-1} are sensitive to variations in the proportions of Si-isotopes, and they inferred that these bands are related to the ν_3 anti-symmetric stretching of the SiO_4 tetrahedra, in which significant Si displacement is expected. They showed that there was significant mixing of ν_1 and

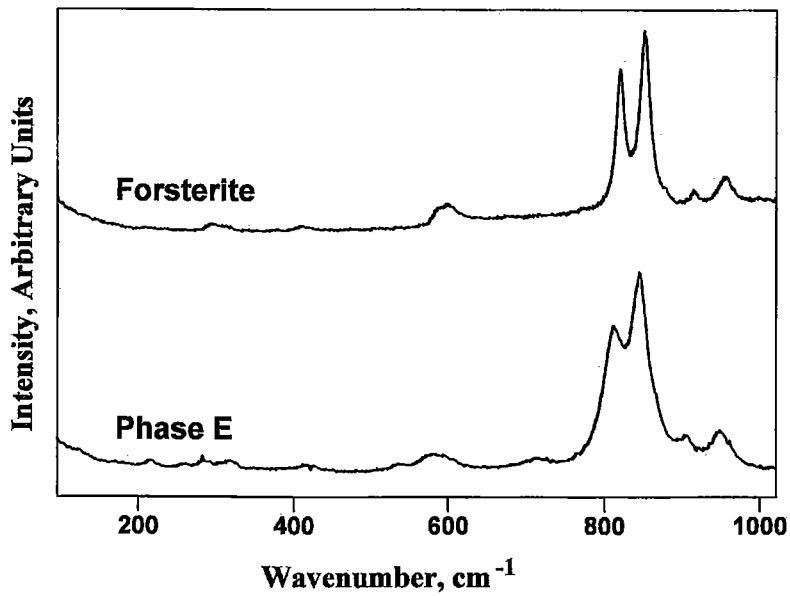

FIG. 4. Comparison of the micro-Raman spectrum in the region 100 to 1020 cm^{-1} for forsterite (top) and phase E (bottom).

ν_3 character for the intense bands at 856 and 824 cm^{-1}. Paques-Ledent & Tarte (1973) also found that infrared bands at 466, 425, 415, 364, 320, 300 and 277 cm^{-1} show large shifts in frequency with Mg-isotope variations, but only small shifts with Si-isotope variations. They inferred that these bands are associated with large translations of Mg atoms and also possibly SiO_4 rotations. All the remaining bands in their experiments seem to involve displacements of both Mg and Si. Therefore, the assignments in Table 2 are based on similar assignments for forsterite as reported by Chopelas (1991).

ACKNOWLEDGEMENTS

We thank Dr. T. Inoue and Professor T. Irifune for providing us with samples of phase E, and Drs. F.C. Hawthorne and R.F. Martin for helpful comments that improved this manuscript. We are grateful to Eric Dowty for providing us with a trial copy of the VIBRATZ program for computing the vibrational spectra of crystals. TPM publishes with the permission of the Executive Director of the Australian Geological Survey Organisation.

REFERENCES

CATTI, M., FERRARIS, G., HULL, S. & PAVESE, A. (1995): Static compression and H disorder in brucite, $Mg(OH)_2$ to 11 GPa: a powder neutron diffraction study. *Phys. Chem. Minerals* **22**, 200-206.

CHOPELAS, A. (1991): Single crystal Raman spectra of forsterite, fayalite, and monticellite. *Am. Mineral.* **76**, 1101-1109.

DOWTY, E. (1987a): Fully automated microcomputer calculation of vibrational spectra. *Phys. Chem. Minerals* **14**, 67-69.

_____ (1987b): Vibrational interactions of tetrahedra in silicate glasses and crystals. II. Calculations on melilites, pyroxenes, silica polymorphs and feldspars. *Phys. Chem. Minerals* **14**, 122-138.

DUFFY, T.S., MEADE, C., FEI, YINGWEI, MAO, HO-KWANG & HEMLEY, R.J. (1995): High-pressure phase transition in brucite, $Mg(OH)_2$. *Am. Mineral.* **80**, 222-230.

FARMER, V.C., ed. (1974): *Infrared Spectra of Minerals*. The Mineralogical Society, London, U.K.

IISHI, K. (1978): Lattice dynamics of forsterite. *Am. Mineral.* **63**, 1198-1208.

INOUE, T., YURIMOTO, H. & KUDOH, Y. (1995): Hydrous modified spinel, $Mg_{1.75}SiH_{0.5}O_4$: a new water reservoir in the mantle transition region. *Geophys. Res. Lett.* **22**, 117-120.

KANZAKI, M. (1989): High pressure phase relations in the system $MgO–SiO_2–H_2O$. *Eos, Trans. Am. Geophys. Union* **70**, 508 (abstr.).

_____ (1991): Stability of hydrous magnesium silicates in the mantle transition zone. *Phys. Earth Planet. Inter.* **66**, 307-312.

KUDOH, Y., FINGER, L.W., HAZEN, R.M., PREWITT, C.T., KANZAKI, M. & VEBLEN, D.R. (1993): Phase E: a high pressure hydrous silicate with unique crystal chemistry. *Phys. Chem. Minerals* **19**, 357-360.

LIEBE, H.C. (1975): Selected terrestrial minerals and their infrared absorption spectral data (4000– 300 cm^{-1}). *In* Infrared and Raman Spectroscopy of Lunar and Terrestrial Minerals (C. Karr, Jr., ed.). Academic Press, London, U.K. (197-229).

LIU, LIN-GUN (1987): Effect of H_2O on the phase behaviour of the forsterite–enstatite system at high pressures and temperatures and implications for the Earth. *Phys. Earth Planet. Inter.* **49**, 142-167.

_____ & MERNAGH, T.P. (1990): Phase transitions and Raman spectra of calcite at high pressures and room temperature. *Am. Mineral.* **75**, 801-806.

_____, _____, LIN, CHUNG-CHERNG & IRIFUNE, T. (1997): Raman spectra of phase E at various pressures and temperatures with geophysical implications. *Earth Planet. Sci. Lett.* **149**, 57-65.

MERNAGH, T.P. & HOATSON, D.M. (1997): Raman spectroscopic study of pyroxene structures from the Munni Munni layered intrusion, Western Australia. *J. Raman Spectrosc.* **28**, 647-658.

_____ & LIU, LIN-GUN (1996): Raman and infrared spectra of hydrous β–Mg_2SiO_4. *Can. Mineral.* **34**, 1233-1240.

OHTANI, E., SHIBATA, T., KUBO, T. & KATO, T. (1995): Stability of hydrous phases in the transition zone and the upper most part of the lower mantle. *Geophys. Res. Lett.* **22**, 2553-2556.

PAQUES-LEDENT, M.T. & TARTE, P. (1973): Vibrational studies of olivine-type compounds. I. The i.r. and Raman spectra of isotropic species of Mg_2SiO_4. *Spectrochim. Acta* **29A**, 1007-1016.

RINGWOOD, A.E. & MAJOR, A. (1967): High-pressure reconnaissance investigations in the system Mg_2SiO_4–MgO–H_2O. *Earth Planet. Sci. Lett.* **2**, 130-133.

ROSSMAN, G.R. (1988): Vibrational spectroscopy of hydrous components. *In* Spectroscopic Methods in Mineralogy and Geology (F.C. Hawthorne, ed.). *Rev. Mineral.* **18**, 193-206.

WILSON, E.B., JR., DECIUS, J.C. & CROSS, P.C. (1980): *Molecular Vibrations. The Theory of Infrared and Raman Vibrational Spectra.* Dover Publications Inc., New York, N.Y.

Received July 15, 1997, revised manuscript accepted October 6, 1998.